



Published in final edited form as:

Prostate. 2012 November ; 72(15): 1638–1647. doi:10.1002/pros.22517.

Hedgehog signaling inhibition by the small molecule Smoothened inhibitor GDC-0449 in the bone forming prostate cancer xenograft MDA PCa 118b

Maria Karlou, PhD¹, Vassiliki Tzelepi, MD, PhD^{1,2}, Sankar Maity, PhD¹, Nora M. Navone, MD, PhD¹, Jun Yang, PhD¹, Anh Hoang¹, Jing-Fang Lu, PhD¹, Christopher J. Logothetis, MD¹, and Eleni Efstathiou, MD, PhD^{1,3,*}

¹Department of Genitourinary Medical Oncology, The David Koch Center for Applied Research of Genitourinary Cancers, The Stanford Alexander Tissue Derivatives Laboratory, The University of Texas MD Anderson Cancer Center, Unit 1374, 1550 Holcombe Boulevard, Houston, TX 77030-4009

²Department of Pathology, Medical School, University of Patras, 26500, Patras, Greece

³Department of Clinical Therapeutics, University of Athens Medical School, Athens, Greece

Abstract

Background—Hedgehog signaling is a stromal-mesenchymal pathway central to the development and homeostasis of both the prostate and the bone. Aberrant Hedgehog signaling activation has been associated with prostate cancer aggressiveness. We hypothesize that Hedgehog pathway is a candidate therapeutic target in advanced prostate cancer. We report aberrant Hedgehog signaling in bone metastatic castrate resistant prostate cancer and we examine the pharmacodynamic effect of Smoothened inhibition in an experimental prostate cancer model.

Methods—Hedgehog signaling was assessed in tissue microarrays of high grade locally advanced and bone metastatic disease. Male SCID mice subcutaneously injected with the bone forming xenograft MDA PCa 118b were treated with GDC-0449. Hedgehog signaling in the tumor microenvironment was assessed by proteomic and species specific RNA expression and compared between GDC-0449 treated and untreated animals.

Results—We observe Hedgehog signaling activation in high grade locally advanced and bone marrow infiltrating disease. Evidence of paracrine activation of Hedgehog signaling in the tumor xenograft, was provided by increased Sonic Hedgehog expression in human tumor epithelial cells, coupled with increased Gli1 and Patched1 expression in the murine stromal compartment, while normal murine stroma didn't exhibit Hh signaling expression. GDC-0449 treatment attenuated Hh signaling as evidenced by reduced expression of Gli1 and Ptch1. Reduction in proliferation (Ki67) was observed with no change in tumor volume.

Conclusions—GDC-0449 treatment is pharmacodynamically effective as evidenced by paracrine Hedgehog signaling inhibition and results in tumor cell proliferation reduction.

*Correspondence to: Eleni Efstathiou, Department of Genitourinary Medical Oncology, Unit 1374, The University of Texas M. D. Anderson Cancer Center, 1550 Holcombe Boulevard, Houston, TX 77030-4009, Office: 7135630894 Fax: 7135639409, eefstathiou@mdanderson.org.

Understanding these observations will inform the clinical development of therapy based on Hedgehog signaling inhibition.

Keywords

Hh signaling; prostate cancer; MDA PCa 118b

Introduction

The microenvironment is integral to prostate carcinogenesis and cancer progression. Microenvironment properties determine the disease phenotype and response to therapy [1]. It thus logically follows that co-targeting the tumor associated microenvironment along with the epithelial component will contribute to disease therapy [2].

Several stromal-epithelial-interacting pathways have been associated with prostate cancer progression and are also implicated in resistance to therapies [1, 3, 4]. Identifying and understanding their role in disease progression will lead to prioritization of therapy targets for further development.

Hedgehog (Hh) signaling plays a diverse and important role in vertebrate development including cell proliferation, differentiation and tissue polarity [5]. Hh signaling also has a physiologic role in tissue regeneration and homeostasis that is mediated by its effect on stromal epithelial interactions. Furthermore it is important in normal prostate and bone development (Fig. 1).

There is emerging evidence that Hh signaling promotes prostate cancer growth and has been identified as a candidate element of disease aggressiveness [6]. It has been proposed to confer growth promoting or survival values in the tumor microenvironment by different mechanisms and to varying degrees as well as to contribute to prostate cancer progression [7, 8]. It may be involved in the predilection of Prostate Cancer (PCa) for bone metastasis, given that bone marrow stromal cells are responsive to Hh ligands. Specifically Indian Hedgehog (Ihh) and Sonic Hedgehog (Shh) stimulate bone regeneration [9, 10]. These reports are consistent with the hypothesis that prostate cancer usurps normal prostate and bone development in progression.

In this work we identify Hedgehog signaling as a shared property in the locally advanced high primary and bone metastatic disease. We then assess the effect of a novel small molecule Hh pathway inhibitor, GDC-0449 in the bone forming xenograft MDA PCa 118b derived from the bone metastasis of a patient with castrate-resistant prostatic adenocarcinoma.

This work is part of a broader effort to develop model systems representative of disease states that will inform the clinical development of individualized microenvironment targeting therapy.

Materials and Methods

Human specimens and tissue microarray (TMA) construction

A tissue microarray was constructed from radical prostatectomy specimens of 70 patients with high grade carcinoma [21 cases with Gleason Score 7 (4+3), 9 cases with Gleason Score 8 and 40 cases with Gleason score 9]. A median of 6 cores (range 6–9) per case was included. Bone marrow biopsies from 67 patients with metastatic PCa were also included. All subjects have given informed consent for the use of the tissue and the study has been approved by the institutional review board of the University of Texas M.D. Anderson Cancer Center. Mean age of patients included in the study was 62 years (SD: 6, range: 46–72).

Immunohistochemistry (IHC)

Four (4) μm tissue sections cut from formalin fixed paraffin embedded tumor xenograft, bone marrow biopsies and TMAs were subjected to immunohistochemical studies.

Immunohistochemical studies were performed using the Dako autostainer (Dako North America Inc., Carpinteria, CA) as described before [2]. Primary antibodies (dilution, company) used included: Ki76 (1:200, Dako, Carpinteria, CA), Shh (H-160, 1:175, Santa Cruz, CA, USA), Smoothed (1:80, Abcam, MA, USA), Patched 1 (1:350, Strategic Diagnostics Inc., DEL, USA), Gli1 (1:300, Novus, CO, USA), Gli2 (1:150, Abcam, MA, USA).

Whole slides of each biomarker were scanned with the Bliss system (Bacus Laboratories Inc, IL, USA) and automatically stored for later retrieval. Epithelial cells were evaluated and subcellular localization of each marker was noted. In the TMA, percentage of positive cells was determined for each core and mean expression was calculated for each case. In the xenografts at least 1000 cells were evaluated and percentage of positive cells was determined. All counts were performed at $\times 400$ magnification. Ki67 was considered as low when expressed in less than 50% of the cells.

Animals

Adult male SCID mice (6–7 weeks, 18–20 g body weight) were purchased from Charles River Laboratories (Wilmington, Mass) and housed 4 per cage under controlled environmental conditions (temperature $22^{\circ}\text{C} \pm 2^{\circ}\text{C}$, 12:12 hour light: dark, with lights on from 06:00am–06:00pm hours). All animals were handled to become adapted for at least 3 days prior to commencing the experiment. All animal experiments were conducted in accordance with accepted standards of animal care and were approved by the Institutional Animal Care and Use Committee of the University of Texas MD Anderson Cancer Center.

Human Prostate Cancer cells MDA PCa 118b

The human prostate cancer cells MDA PCa 118b were derived from the bone metastasis of a patient with castrate-resistant prostatic adenocarcinoma. These cells induce robust osteoblastic reactions in the bone and subcutis of immunodeficient mice. They have loss of androgen receptor, prostate-specific antigen (PSA) and prostate acid phosphatase (PAP)

expression and are capable of developing tumors after subcutaneous or intraprostatic injection.

For tumor analysis, we implanted into subcutaneous pockets of 6- to 8-week-old male CB17 SCID mice (Charles River Laboratories) small pieces of MDA PCa 118b tumor. We then harvested the tumor after 3 weeks of treatment. Tumor was divided in two parts; one was flash frozen and used for RNA and protein extraction and the second one after being decalcified in formic acid, was processed for histological and immunohistochemical analysis.

Hedgehog pathway inhibitor treatment

GDC-0449, which was a kind gift from Genentech, CA is a small-molecule antagonist of the Hh signaling pathway with a molecular weight of approximately 450 g/mol. It inhibits signaling by Smoothed (Smo), downstream of ligand binding, as well as the majority of the known pathway-activating mutations. GDC-0449 binds to and inhibits Smo that results in blocking of the Hh signal.

Animals were randomized to oral gavage, twice a day for a total of 21 days with either control vehicle or 100 mg/kg from a 10mg/ml solution in 0.5% methylcellulose (MCT 0.5 mmol/kg). Bone formation before the beginning of the treatment was assessed by X-Ray analysis. They were divided into two groups of 8 animals each: control group and treatment group according to tumor volume measurement on day 12 after implantation. Mean tumor volume per group was $180\text{mm}^3 \pm 20\text{mm}^3$. Tumor volumes using a caliper and the formula $(L \times W \times H)/2 \times 4/3 \times 3.14$ and body weights were measured twice weekly during the 21 days of Hh pathway inhibition treatment with GDC-0449.

RNA isolation

Total RNA was extracted from fresh-frozen OCT blocks by using an RNeasy Mini Kit (Qiagen Inc., Valencia, CA) according to the manufacturer's instructions. Genomic DNA was eliminated by a DNase on-column treatment with an RNase-free DNase set (Qiagen). Total RNA was eluted in RNase-free water, and the concentration was calculated by determining absorbance at 260 nm (Ultraspec 2000; Pharmacia Biotech Uppsala, Sweden).

Reverse-transcription and quantitative real-time PCR (qRT-PCR)

Total RNA was reverse transcribed to single-stranded cDNA using Superscript II Reverse Transcriptase (Invitrogen Corp., Carlsbad, CA) according to the manufacturer's instructions. qRT-PCR amplifications were performed in Optical 96-well plates (Applied Biosystems, Inc., Foster City, CA). All standards and samples were run in triplicate using an MX3000P analyzer (Agilent Technologies, Inc., Santa Clara, CA), and the mean result was obtained for use in further calculations. The transcript level of glyceraldehyde-3-phosphatase dehydrogenase (GAPDH) was assayed simultaneously as an internal control to normalize transcript levels of genes of interest. Baseline and threshold values were automatically determined for all plates using MXPro QPCR software. We transformed raw cycle threshold (Ct) values to quantities by using a Microsoft Excel (Microsoft Corp., Redmond, WA) spreadsheet we generated on the basis of the comparative Ct method. The resulting data

were converted into correct input files, according to the requirements of the software. Epithelial and stromal expression of components could be discriminated by human-specific and mouse-specific primers, respectively (Table I).

Protein extraction-Western blots

Frozen tumor tissue was used for protein extraction using lysis buffer with protease inhibitors set on ice. Homogenization of the tumor tissue by electric homogenizer for 8 seconds was followed by centrifugation at 4°C, 14.000 rpm for 10 minutes. Protein concentration was determined by BCA reaction.

Western blotting was performed as previously described [10], while nitrocellulose membranes were incubated with 1:250, 1:10.000 and 1:500 goat polyclonal anti-Ptch1, rabbit polyclonal anti-Gli1, and anti-SuFu respectively, followed by 1:3000 horseradish peroxidase-conjugated donkey antigoat/antirabbit IgG (Santa Cruz, catalog number SC2020) and developed by enhanced chemiluminescence (Amersham Corp.)

Statistics

For analysis of differences between groups we used 2-sample *t* tests. *P* values of less than 0.05 were considered statistically significant. Correlations between the expression of the studied markers was analysed with Pearson's correlation test.

Results

Hh signaling is active in human aggressive primary and bone metastatic disease

Hh signaling components expression was noted in the microenvironment of high grade primary and bone marrow metastatic prostate cancer. Expression of Shh, Gli2 and Gli1 was high in both primary high grade prostate cancer and castrate resistant bone marrow metastases. Ptch expression was higher in bone marrow metastases compared to primary prostate cancer tumors ($p=0.001$, Table II, Fig. 2).

Hh pathway is active in the MDA PCa 118b xenograft model microenvironment but not in normal mouse stroma

We first tested for expression of Hh pathway components expression in normal mouse derived stroma and then in mouse derived stroma after MDA PCa 118b tumor implantation and growth. Hh pathway components expression as assessed by qRT-PCR was significantly lower or undetectable in normal mouse derived stroma compared to stroma following tumor implantation (Table III). This indicates that Hh signaling pathway is activated as a result of xenograft implantation supporting the tumor microenvironment specific paracrine pathway activation.

Within the tumor microenvironment, Shh expression in tumor epithelial cells was significantly higher compared to stromal compartment by 70-fold ($p<0.0001$, $n=3$), assessed by human gene-specific primers and mouse gene-specific primers respectively (Fig. 3 A). Gli1 expression in the stromal compartment was higher compared to human tumor cells by

20-fold ($p=0.049$, $n=3$, Fig. 3 A). This further supports the paracrine interaction between tumor epithelium and stroma within the microenvironment.

Morphological characterization of prostate cancer xenograft MDA PCa 118b

All MDA PCa 118b prostate cancer xenografts displayed the morphologic features previously described [11]. Briefly, the tumor cells were arranged in solid sheets and nodules with rare gland formations, had medium sized nuclei with prominent nucleoli and moderate amounts of cytoplasm. An intense osteoblastic reaction with the formation of a bone-like extracellular matrix was noted in the stroma of the tumors. There was no significant difference between the treated and the untreated group in terms of tumor morphology, amount of necrosis, mitotic rate and bone-like stroma formation as determined by histopathological analysis of H&E stained sections (Fig. 3 B, C).

GDC-0449 inhibits Hh signaling

We performed qRT-PCR analysis of Shh, Gli1, Gli2, Smo, Ptch1 and Sufu in GDC-0449 treated and untreated groups. Stromal expression of Gli1 and Ptch1, assessed by mouse gene-specific primers, was marginally lower in the treated group compared to the control (Table IV). Given that Gli1 and Ptch1 are reliable markers of an active Hh pathway these results confirm the pharmacodynamic effect of GDC-0449. Expression of Gli2 and Shh followed the same trend (Table IV).

Tumor epithelial expression of Sufu was significantly lower in treated than in untreated controls. Immunohistochemical testing confirmed a decrease in Sufu expression in the tumor epithelium (data not shown). A trend for lower epithelial Smoothed expression was not statistically significant given the heterogeneity across the group (Table IV). This included differences in both mRNA and protein assessment of expression of Hh signaling components.

Paracrine activity of the pathway is further supported by the correlation identified between the Shh ligand expression in the tumor epithelium and the pathway components Gli1 and Ptch1 stromal expression ($p=0.001$, $r=0.994$ and $p=0.001$, $r=0.992$ respectively, see below).

Hh pathway components expression

Correlations between the markers—Significant correlations between the mRNA expression levels of the Hh signaling components were found in the control group. These were observed both within the epithelial- [**Smoothed-Gli1** ($p=0.004$, $r=0.996$), **Ptch1-Shh** ($p=0.013$, $r=0.904$)] and the stromal [**Shh-Ptch1**, $p=0.045$, $r=0.955$), **Sufu-Gli2** ($p=0.003$, $r=0.981$), **Gli1-Ptch1** ($p=0.004$, $r=0.978$)] compartments, but also between the epithelial and the stromal compartment [**Shh (epithelium)-Gli1 (stroma)** ($p=0.001$, $r=0.994$), **Ptch1 (epithelium)-Gli1 (stroma)** ($p=0.01$, $r=0.958$), **Shh (epithelium)-Ptch1 (stroma)** ($p=0.001$, $r=0.992$), **Ptch1 (epithelium)-Ptch1 (stroma)** ($p=0.043$, $r=0.89$)].

In the treated group, fewer correlations were noted: **Ptch1 (epithelium)-Sufu (stroma)** ($p=0.013$, $r=0.907$), **Ptch1 (epithelium)-Ptch1 (stroma)** ($p=0.006$, $r=0.938$), **Ptch1 (stroma)-Sufu (stroma)** ($p=0.047$, $r=0.818$). Importantly no correlation between ligand

expression and pathway activation was noted neither in the epithelium nor in the stromal compartment or between the epithelium and the stroma.

Prostate cancer xenograft MDA PCa 118b Volume and Immunohistochemistry

—Assessment of protein expression of markers of interest by IHC is depicted in Table IV. The epithelial component between the treated and the control group had no difference in assessed pathway components by qRT-PCR. Additionally, and consistent with the absence of differences in tumor volume, there was no difference in the proliferation rate, as determined by Ki67 immunohistochemistry, between the treated and the control group.

We explored likely correlations between the level of Hh pathway activation and Ki67 expression. Interestingly, in the treated group, lower proliferation rate correlated with lower Gli2 mRNA in the stromal cells ($p=0.04$) and higher Gli2 mRNA expression in the malignant cells ($p<0.001$). In the control group, no correlation between the proliferation rate and the mRNA expression of the markers tested was noted. However, high nuclear expression of Gli2 protein was marginally correlated with high Ki67 expression (Fig. 4 A, B), since mean \pm SD of Gli2 expression for the cases with low Ki67 was 20 \pm 29% whereas for the cases with high Ki67 it was 80 \pm 28% ($p=0.094$). These results might imply that downregulation of the Hh pathway in the stromal and not in the epithelial compartment of the tumor reduces cancer cell proliferation rate, further supporting a paracrine mode of action of Hh pathway inhibition in prostate cancer.

No significant tumor volume differences were found between treated and untreated group of MDA PCa 118b mouse model (Fig. 4 C) yet a trend for slower tumor growth in the treated group was recorded.

Discussion

Hedgehog signaling has been proposed as a therapy target in prostate cancer based on several lines of preclinical evidence. Aberrant pathway activation has been implicated in prostate carcinogenesis and specifically the aggressive phenotype of the disease [6, 12, 13, 14]. The clinical relevance of these findings is supported by aberrant Hh signaling in PCa progression [2, 15].

In this work we confirm aberrant Hh signaling in locally advanced high grade disease as previously reported and also report similar signaling activity in bone marrow infiltrating castrate resistant prostate cancer (CRPC) [14, 15]. We further observe a correlation between Shh ligand expression in the prostate cancer cells and activation of Hh signaling as evidenced by increased Gli1 and Ptch1, both reliable markers of pathway activity, in the stroma. Expression levels of Shh responsive target genes Gli1 and Ptch1, in the stromal compartment of the xenografts was higher as compared to the epithelium suggesting that Hh ligands produced by the cancer, activate the pathway in the adjacent stroma. Of note, mouse stroma from non-tumor injected animals exhibits nearly undetectable Gli1 and Ptch1 expression supporting the tumor microenvironment specific paracrine property of Hh signaling. Our findings parallel those reported by other in tumor microenvironment disease setting including pancreatic carcinogenesis [16, 17].

Currently small molecule Hh pathway antagonists are being tested as candidate anticancer drugs in tumors where aberrant Hh signaling plays a central role in carcinogenesis as is the case for basal cell carcinoma and medulloblastoma. GDC-0449 initial clinical outcome in basal cell carcinoma is quite promising [18]. Moreover in a case of medulloblastoma, a malignancy known to be driven by constitutive Hh pathway signaling, treatment with GDC-0449 was well tolerated and had benefits, albeit transient, for the subject [19].

The pharmacodynamic effect of the reagent was confirmed by Hh signaling attenuation. Oral administration of Hh antagonist GDC-0449 to mice harbouring human prostate MDA PCa 118b cancer xenografts resulted in the down regulation of the expression of Hh target genes, namely Gli1 and Ptch1, in the stromal microenvironment. These data parallels human tissue based data suggesting that Hh activity mainly ensues in the stromal compartment. This is consistent with a paracrine signaling mechanism, where Hh ligands produced by tumor epithelial cells activate aberrant pathway signaling in the stromal compartment and thus a cascade of events supportive of tumor survival in the microenvironment ensues. This was accompanied by a decrease in tumor cell proliferation rate though no significant effect on tumor volume was observed. A trend for slower tumor growth following treatment was observed yet results were likely limited by the small number of animals treated and short duration of treatment. Similar results were reported for the small molecule Hh antagonist IPI-269609 on pancreatic cancer [20]. We agree with the investigators suggesting that optimization of dosing and schedule for an animal model may need to be further explored. More importantly given the proposed mechanism of action through circumventing microenvironment support it is quite likely that Hh signaling inhibition should be combined with an epithelial targeting reagent.

These findings are in line with our clinical experience where the initial suppression of Hh signaling by thalidomide had no effect on tumor size in the locally advanced disease setting though it was accompanied by PSA reduction and trend for slower proliferation rate [2].

More importantly Hh signaling in common adult solid tumors is a complex signaling network with possible interplay involving numerous signaling pathways such as Wnt/b catenin, FGF, Notch, TGF-b/BMP, androgen receptor and others [21]. Thus combinatorial targeting is a rational approach and may include both direct epithelial compartment targeting with cytotoxic agents and stromal-epithelial inhibition necessary to achieve maximised benefit [22, 23].

Conclusions

Hh signaling demonstrates paracrine activation in the MDA PCa 118b prostate cancer xenograft model and the Smoothened inhibitor GDC-0449 effectively inhibits pathway activation. This pharmacodynamic effect is coupled with a decline in tumor epithelial cell proliferation. These findings propose an attractive therapeutic strategy consisting of coupling Hh signaling inhibition with traditional therapies in order to enhance the curative efficacy of anticancer treatment. To address the impetus for informative clinical investigation we are currently performing a preoperative trial in high risk locally advanced prostate cancer combining short Hedgehog signaling pathway inhibition with androgen ablation.

Acknowledgments

We thank Kim-Anh T. Vu at the University of Texas, M.D. Anderson Cancer Center for her assistance in preparing the graphic art.

Supported by the Young Investigator Award Prostate Cancer Foundation

References

1. Josson S, Matsuoka Y, Chung LW, Zhau HE, Wang R. Tumor-stroma co-evolution in prostate cancer progression and metastasis. *Semin Cell Dev Biol.* 2010; 21(1):26–32. [PubMed: 19948237]
2. Efstathiou E, Troncoso P, Wen S, Do KA, Pettaway CA, Pisters LL, McDonnell TJ, Logothetis CJ. Initial modulation of the tumor microenvironment accounts for thalidomide activity in prostate cancer. *Clin Cancer Res.* 2007; 13(4):1224–1231. [PubMed: 17317833]
3. Basanta D, Strand DW, Lukner RB, Franco OE, Cliffl DE, Ayala GE, Hayward SW, Anderson AR. The role of transforming growth factor-beta-mediated tumor-stroma interactions in prostate cancer progression: an integrative approach. *Cancer Res.* 2009; 69(17):7111–7120. [PubMed: 19706777]
4. Cano P, Godoy A, Escamilla R, Dhir R, Onate SA. Stromal-epithelial cell interactions and androgen receptor-coregulator recruitment is altered in the tissue microenvironment of prostate cancer. *Cancer Res.* 2007; 67(2):511–519. [PubMed: 17234758]
5. Varjosalo M, Taipale J. Hedgehog: functions and mechanisms. *Genes Dev.* 2008; 22(18):2454–2472. [PubMed: 18794343]
6. Karhadkar SS, Bova GS, Abdallah N, Dhara S, Gardner D, Maitra A, Isaacs JT, Berman DM, Beachy PA. Hedgehog signalling in prostate regeneration, neoplasia and metastasis. *Nature.* 2004; 431(7009):707–712. [PubMed: 15361885]
7. Scales SJ, de Sauvage FJ. Mechanisms of Hedgehog pathway activation in cancer and implications for therapy. *Trends Pharmacol Sci.* 2009; 30(6):303–312. [PubMed: 19443052]
8. Tzelepi V, Efstathiou E, Wen S, Troncoso P, Karlou M, Pettaway CA, Pisters LL, Hoang A, Logothetis CJ, Pagliaro LC. Persistent, biologically meaningful prostate cancer after 1 year of androgen ablation and docetaxel treatment. *J Clin Oncol.* 2011; 29(18):2574–2581. [PubMed: 21606419]
9. Edwards PC, Ruggiero S, Fantasia J, Burakoff R, Moorji SM, Paric E, Razzano P, Grande DA, Mason JM. Sonic hedgehog gene-enhanced tissue engineering for bone regeneration. *Gene Ther.* 2005; 12(1):75–86. [PubMed: 15510177]
10. Karp SJ, Schipani E, St-Jacques B, Hunzelman J, Kronenberg H, McMahon AP. Indian hedgehog coordinates endochondral bone growth and morphogenesis via parathyroid hormone related-protein-dependent and -independent pathways. *Development.* 2000; 127(3):543–548. [PubMed: 10631175]
11. Li ZG, Mathew P, Yang J, Starbuck MW, Zurita AJ, Liu J, Sikes C, Multani AS, Efstathiou E, Lopez A, Wang J, Fanning TV, Prieto VG, Kundra V, Vazquez ES, Troncoso P, Raymond AK, Logothetis CJ, Lin SH, Maity S, Navone NM. Androgen receptor-negative human prostate cancer cells induce osteogenesis in mice through FGF9-mediated mechanisms. *J Clin Invest.* 2008; 118(8):2697–2710. [PubMed: 18618013]
12. Sanchez P, Hernández AM, Stecca B, Kahler AJ, DeGueme AM, Barrett A, Beyna M, Datta MW, Datta S, Ruiz i Altaba A. Inhibition of prostate cancer proliferation by interference with SONIC HEDGEHOG-GLI1 signaling. *Proc Natl Acad Sci USA.* 2004; 101(34):12561–12566. [PubMed: 15314219]
13. Kim TJ, Lee JY, Hwang TK, Kang CS, Choi YJ. Hedgehog signaling protein expression and its association with prognostic parameters in prostate cancer: A retrospective study from the view point of new 2010 anatomic stage/prognostic groups. *J Surg Oncol.* 2011 Jun 7. doi: 10.1002/jso.21988
14. Tzelepi V, Karlou M, Wen S, Hoang A, Logothetis C, Troncoso P, Efstathiou E. Expression of hedgehog pathway components in prostate carcinoma microenvironment: shifting the balance towards autocrine signaling. *Histopathology.* 2011; 58(7):1037–1047. [PubMed: 21707705]

15. Azoulay S, Terry S, Chimingqi M, Sirab N, Faucon H, Gil Diez de Medina S, Moutereau S, Maillé P, Soyeux P, Abbou C, Salomon L, Vacherot F, de La Taille A, Loric S, Allory Y. Comparative expression of Hedgehog ligands at different stages of prostate carcinoma progression. *J Pathol.* 2008; 216(4):460–470. [PubMed: 18825689]
16. Tian H, Callahan CA, DuPree KJ, Darbonne WC, Ahn CP, Scales SJ, de Sauvage FJ. Hedgehog signaling is restricted to the stromal compartment during pancreatic carcinogenesis. *Proc Natl Acad Sci USA.* 2009; 106(11):4254–4259. [PubMed: 19246386]
17. Fan L, Pepicelli CV, Dibble CC, Catbagan W, Zarycki JL, Laciak R, Gipp J, Shaw A, Lamm ML, Munoz A, Lipinski R, Thrasher JB, Bushman W. Hedgehog signaling promotes prostate xenograft tumor growth. *Endocrinology.* 2004; 145(8):3961–3970. [PubMed: 15132968]
18. Von Hoff DD, LoRusso PM, Rudin CM, Reddy JC, Yauch RL, Tibes R, Weiss GJ, Borad MJ, Hann CL, Brahmer JR, Mackey HM, Lum BL, Darbonne WC, Marsters JC Jr, de Sauvage FJ, Low JA. Inhibition of the hedgehog pathway in advanced basal-cell carcinoma. *N Engl J Med.* 2009; 361(12):1164–1172. [PubMed: 19726763]
19. Rudin CM, Hann CL, Larterra J, Yauch RL, Callahan CA, Fu L, Holcomb T, Stinson J, Gould SE, Coleman B, LoRusso PM, Von Hoff DD, de Sauvage FJ, Low JA. Treatment of medulloblastoma with hedgehog pathway inhibitor GDC-0449. *N Engl J Med.* 2009; 361(12):1173–1178. [PubMed: 19726761]
20. Feldmann G, Fendrich V, McGovern K, Bedja D, Bisht S, Alvarez H, Koorstra JB, Habbe N, Karikari C, Mullendore M, Gabrielson KL, Sharma R, Matsui W, Maitra A. An orally bioavailable small-molecule inhibitor of Hedgehog signaling inhibits tumor initiation and metastasis in pancreatic cancer. *Mol Cancer Ther.* 2008; 7(9):2725–2735. [PubMed: 18790753]
21. Teglund S, Toftgård R. Hedgehog beyond medulloblastoma and basal cell carcinoma. *Biochim Biophys Acta.* 2010; 1805(2):181–208. [PubMed: 20085802]
22. Chung LW, Huang WC, Sung SY, Wu D, Otero-Marah V, Nomura T, Shigemura K, Miyagi T, Seo S, Shi C, Moliterno J, Elmore J, Anderson C, Isotani S, Edlund M, Hsieh CL, Wang R, Shehata B, Zhau HE. Stromal-epithelial interaction in prostate cancer progression. *Clin Genitourin Cancer.* 2006; 5(2):162–170. [PubMed: 17026806]
23. Mimeault M, Batra SK. Frequent Gene Products and Molecular Pathways Altered in Prostate Cancer- and Metastasis-Initiating Cells and their Progenies and Novel Promising Multitargeted Therapies. *Mol Med.* 2011 May 20. doi: 10.2119/molmed.2011.00115

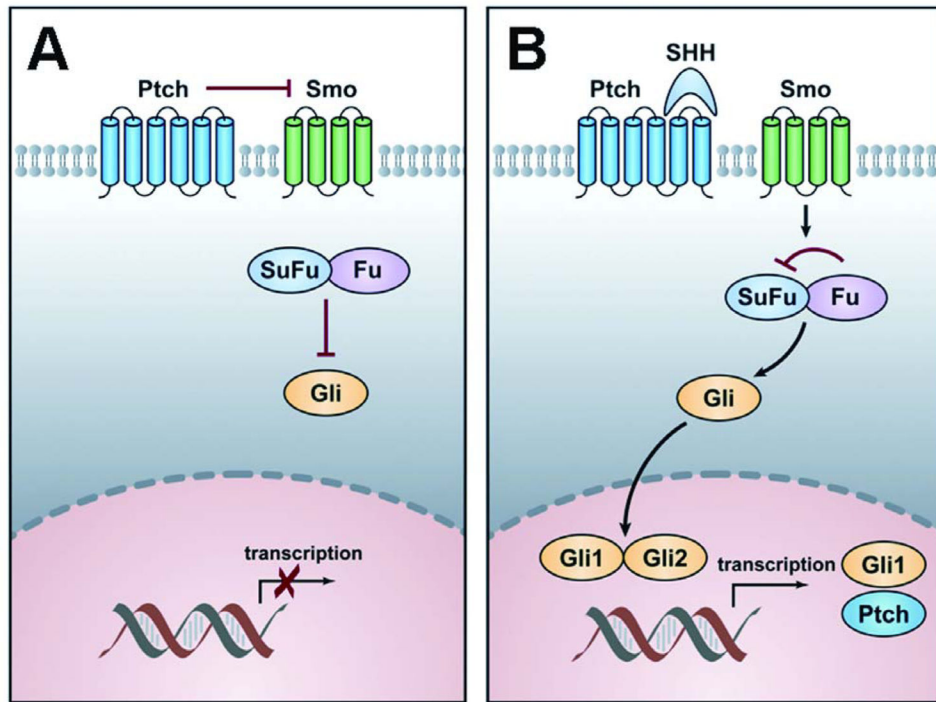


Figure 1. Schematic diagram of the Hh pathway

A: In the absence of ligand, the transmembrane receptor Patched (Ptch) normally inhibits the signaling function of another transmembrane protein, Smoothened (Smo), thereby blocking the expression of target genes. In that inactive situation, Suppressor of Fused (SuFu) prevents Gli from translocating to the nucleus.

B: In the presence of the ligand Sonic Hedgehog (Shh), the repression of Smo is relieved after binding of Shh to Ptch. Smo further transduces a signal resulting in the release of transcription factor Gli from the cytoplasmic proteins Fused (Fu) and SuFu. In the active situation SuFu is inhibited by Fu and Gli is released, translocates to the nucleus and activates target genes transcription, such as Ptch and Gli1.

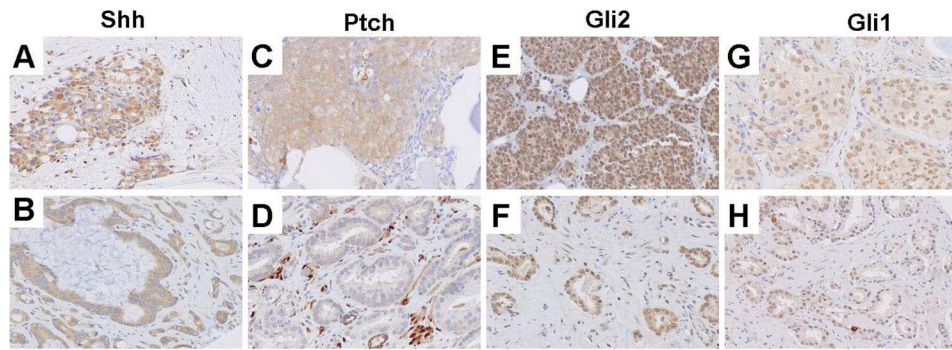


Figure 2. Expression of Shh pathway components in bone marrow metastatic (A,C,E,G) and primary (B,D,F,H) prostate cancer

Expression of Shh is high in both metastatic (A) and primary (B) prostate cancer. Ptch expression is higher in bone marrow metastasis (C) compared to primary prostate cancer (D). High expression of Gli2 and Gli1 is noted in metastatic and primary prostate cancer (E–H) (original magnification $\times 200$).

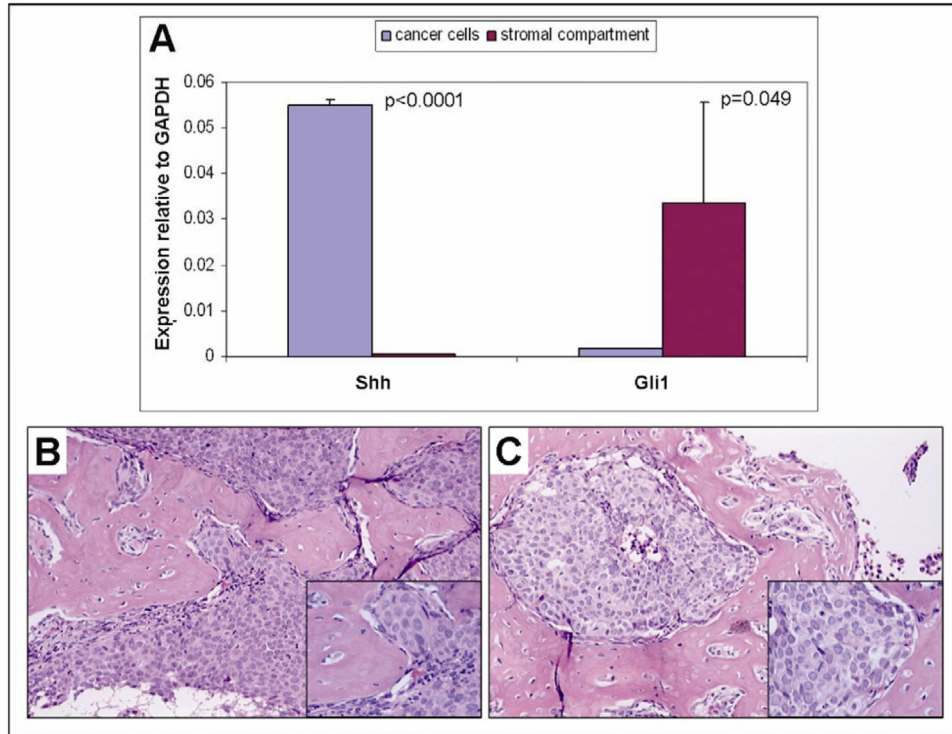


Figure 3. Upregulated epithelial Shh and stromal Gli1 mRNA expression and MDA PCa 118b tumor morphology

A. Mean Shh and Gli1 mRNA expression levels in cancer cells and in stromal compartment of MDA PCa 118b prostate cancer xenograft. B. Control and C. Treated tumors display similar histopathologic features and are characterized by robust metaplastic bone formation (H&E, original magnification $\times 100$, inset: original magnification $\times 200$).

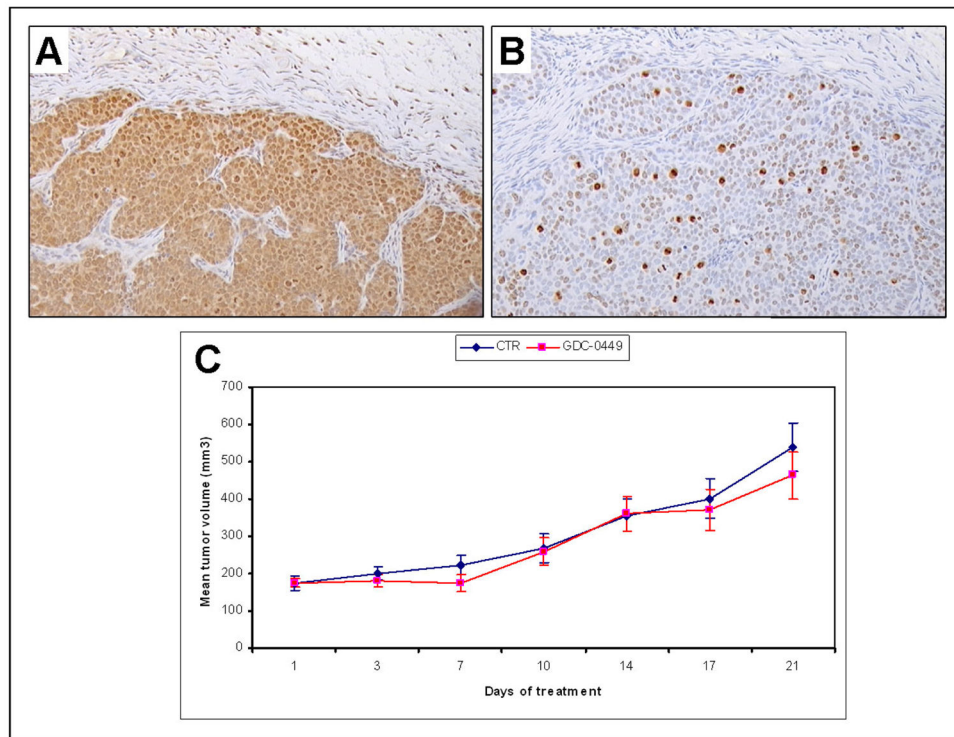


Figure 4. A. Gli2 and B. Ki67 expression, C. Mean tumor volume of MDA PCa 118b xenograft
 A. High expression of Gli2 in a tumor treated with GDC-0449 (original magnification $\times 100$). B. High expression of ki67 in the same tumor as A (original magnification $\times 100$). C. Mean tumor volume of MDA PCa 118b prostate cancer xenograft during 21 days of treatment with small molecule Smo inhibitor GCD-0449. Control group with blue and GDC-0449 treated group with red color.

Table I

Sequences (5'-3') of primers used in qRT-PCR analysis of human (h) and mouse (m) gene expression.

Gene	Forward Primer	Reverse Primer
hGAPDH	CCA CAT CGC TCA GAC ACC AT	GCA ACA ATA TCC ACT TTA CCA GAG TTA A
hShh	AAG GAC AAG TTG AAC GCT TTG G	TCG GTC ACC CGC AGT TTC
hGli1	AAT GCT GCC ATG GAT GCT AGA	GAG TAT CAG TAG GTG GGA AGT CCA TAT
hSufu	CGG AGG GGA GAG ACC ATA TT	CAC TTG GCA CTG ACA CCA CT
hSmo	ACC TAT GCC TGG CAC ACT TC	GTG AGG ACA AAG GGG AGT GA
hPTCH1	TCA ACT GGA ACG AGG ACA AA	CAC CTT TTG AGT GGA GTT CT
mGAPDH	AGA ACA TCA TCC CTG CAT CC	CAC ATT GGG GGT AGG AAC AC
mShh	AAT GCC TTG GCC ATC TCT GT	GCT CGA CCC TCA TAG TGT AGA GAC T
mGli1	GGA AGT CCT ATT CAC GCC TTG A	CAA CCT TCT TGC TCA CAC ATG TAA G
mPtch1	CTC TGG AGC AGA TTT CCA AGG	TGC CGC AGT TCT TTT GAA TG
mGli2	CCT TCT CCA ATG CCT CAG AC	GGG GTC TGT GTA CCT CTT GG
mSufu	GGT CCC TGG CTG ATA ACT GA	CCG TCT GTC TCA ATG CCT TT

Table II

Mean expression levels of Hh pathway components in high grade and bone marrow metastatic PCa.

	High grade PCa (n=70, mean±SD)	Bone Marrow Infiltrating CRPC (n=67, mean±SD)	p-value
Shh	80±24	80±22	0.059
Ptch	30±26	50±36	0.001
Smo	90±14	90±19	0.317
Gli1	70±30	75±30	0.148
Gli2	60±32	90±20	<0.001

Author Manuscript

Author Manuscript

Author Manuscript

Author Manuscript

Table III

mRNA expression of Hh pathway components in normal stroma and stroma after MDA PCa 118b tumor implantation.

	Normal stroma (mean±SD)	Stroma after MDA PCa 118b tumor implantation (mean±SD)	p-value
Sufu	0.044±0.02	60.18±33.09	0.02
Gli1	0.29±0.19	445.73±363.03	0.04
Gli2	0.075±0.01	266.545±215.92	0.03
Shh	undetectable	0.237±0.21	-
Ptch1	1.42±0.35	2846.54±279.1	0.04

Author Manuscript

Author Manuscript

Author Manuscript

Author Manuscript

Table IV

Expression of Hh pathway components and Ki67 in stromal and cancer cells in the GDC-0449 treated and control groups of MDA PCa 118b xenograft (mean±SD, CTR: control group).

	Stromal Cells	GDC-0449	CTR	p-value
RNA (mean±SD)	<i>Sufu</i>	110.77±89.43	60.18±33.09	0.2645
	<i>Gli1</i>	139.81±129.49	445.73±363.03	0.0845
	<i>Gli2</i>	140.03±86.57	266.545±215.92	0.2180
	<i>Shh</i>	0.164±0.13	0.237±0.21	0.5298
	<i>Ptch1</i>	303.11±182.28	2846.54±279.1	0.0509
	Cancer Cells			
	<i>Sufu</i>	1.33±0.71	2.69±0.94	0.018
	<i>Gli1</i>	2.338±2.5	2.14±3.2	0.9178
	<i>Shh</i>	198.343±55.93	237.21±103.78	0.473
	<i>Ptch1</i>	150.78±109.4	124.38±31.93	0.583
	<i>Smo</i>	0.388±0.135	1.73±2.7	0.2483
Protein (IHC)	Cancer Cells			
	<i>Shh</i>	100±0	100±9	0.297
	<i>Smoothened</i>	40±41	30±36	0.577
	<i>Gli2 (nuclear)</i>	30±26	40±49	0.630
	<i>Gli2 (cytoplasmic)</i>	90±12	100±0	0.254
	<i>Ki67</i>	60±31	30±38	0.292